

---

Proceedings of the International School and Conference on Optics and Optical Materials, ISCOM07, Belgrade, Serbia, September 3–7, 2007

## The Effects of Nonstoichiometry on Optical Properties of Oxide Nanopowders

M. ŠĆEPANOVIĆ<sup>a</sup>, M. GRUJIĆ-BROJČIN<sup>a,\*</sup>,  
Z. DOHČEVIĆ-MITROVIĆ<sup>a</sup>, K. VOJISAVLJEVIĆ<sup>b</sup>,  
T. SREĆKOVIĆ<sup>b</sup> AND Z.V. POPOVIĆ<sup>a</sup>

<sup>a</sup>Center for Solid State Physics and New Materials  
Institute of Physics, Pregrevica 118, 11080 Belgrade, Serbia  
<sup>b</sup>Institute of Multidisciplinary Research, Kneza Višeslava 1,  
Belgrade, Serbia

In this paper we illustrate the change of optical properties of mechanically activated wurtzite ZnO powder and laser synthesized anatase TiO<sub>2</sub> nanopowder due to the nonstoichiometry caused by mechanical activation and/or laser irradiation in vacuum. Both of the investigated materials are widely used in optoelectronics and the examination of their optical properties under different preparation and environmental conditions is of great practical interest.

PACS numbers: 77.84.Bw, 73.63.Bd, 78.67.-n, 78.55.-m, 78.30.-j

### 1. Introduction

The high surface-to-volume ratio of nanocrystals suggests that the surface properties have significant effects on their structural and optical properties. This could be related to the presence of gap surface states arising from surface nonstoichiometry, unsaturated bonds, etc. [1]. Therefore the investigation and control of the surface processes is an important step toward understanding the optical properties of oxide nanocrystals.

Optical properties of as prepared and laser irradiated mechanically activated ZnO powder and laser synthesized anatase TiO<sub>2</sub> nanopowder were investigated by photoluminescence (PL) and Raman spectroscopy. The spectra excited by different lines of Ar<sup>+</sup> and He–Cd lasers at room temperatures in air and vacuum are compared.

### 2. Experiment

A commercial ZnO powder (Kemika, p.a. 99.96%) was mechanically activated by grinding in a vibro-mill with steel rings. The grinding time was

---

\*corresponding author; e-mail: myramyra@phy.bg.ac.yu

30 and 300 minutes and the powders are labeled as ZnO(30) and ZnO(300), respectively. Average crystallite size obtained from X-ray diffraction (XRD) results are: 190 nm for ZnO(0), 106 nm for ZnO(30), and 44 nm for ZnO(300) [2]. Anatase TiO<sub>2</sub> nanopowder was synthesized by laser-induced pyrolysis, using titanium isopropoxide as a liquid precursor. The produced powder was calcined in air for 4 h at 500°C, and its average crystallite size obtained from XRD was about 18 nm.

Raman measurements were performed in the backscattering geometry using the 457.9 nm of Ar<sup>+</sup> and 442 nm line of HeCd laser, Jobin-Yvon U1000 monochromator and a photomultiplier as a detector. PL spectra were excited by 457.9 nm of Ar<sup>+</sup> laser, as well as UV (325 nm) and visible (442 nm) lines of a He–Cd laser, using the same equipment as in the Raman measurements. All experiments are performed at room temperature in air and vacuum.

### 3. Results and discussion

#### 3.1. ZnO

Raman spectra taken on non-activated ZnO powder (ZnO(0)) in air and vacuum are shown in Fig. 1, where the observed first-order Raman modes are assigned

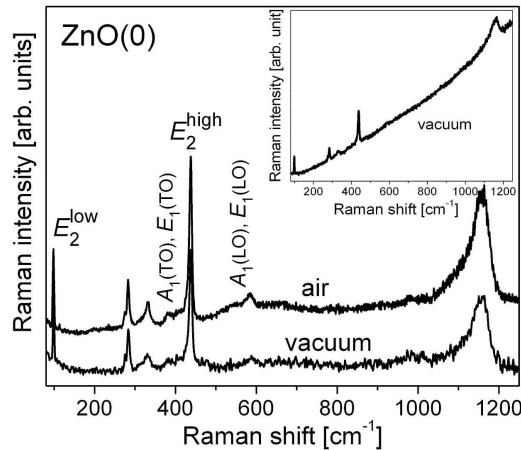


Fig. 1. Raman spectra of nonactivated ZnO powder in air and vacuum. The original Raman spectrum in vacuum before subtraction of background due to the luminescence is shown in the inset.

to the Raman spectrum of wurtzite ZnO [3, 4]: 100 ( $E_2^{\text{low}}$ ), 383 ( $A_1(\text{TO})$ ), 409 ( $E_1(\text{TO})$ ), 438.4 ( $E_2^{\text{high}}$ ), 543 ( $A_1(\text{LO})$ ), and 585 ( $E_1(\text{LO})$ ). Additionally, several second-order Raman modes positioned at 331, 776, 984, 1112, and 1159  $\text{cm}^{-1}$  were found. Two additional modes at 275 and 284  $\text{cm}^{-1}$  are related to intrinsic host lattice defects [2]. The spectrum in vacuum is obtained by subtracting background due to the luminescence from the original spectrum (inset). It is obvious that there is no substantial change in the position and shape of the Raman modes after

irradiation in vacuum. Also there are no additional changes in mode behavior in the Raman spectra of activated samples due to irradiation in vacuum, but those ascribed to the tensile strain introduced by activation [2].

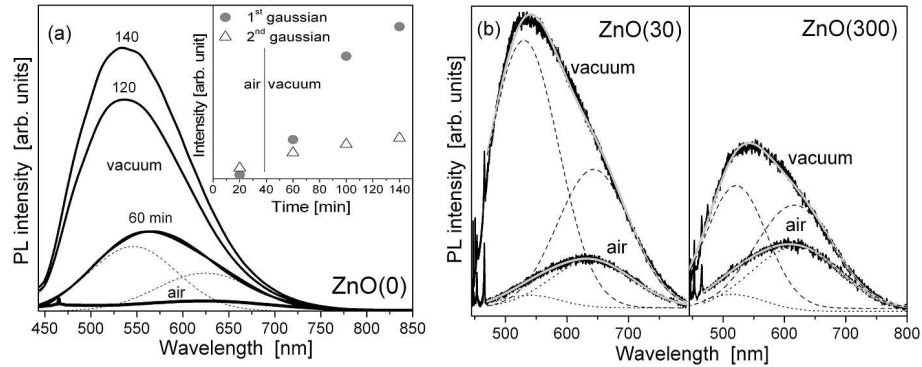


Fig. 2. PL spectra excited by 442 nm He–Cd laser line of (a) nonactivated and (b) activated for 30 and 300 min ZnO powder in air and vacuum, fitted to the sum of two Gaussians. Time dependences of Gaussian intensities of nonactivated ZnO are shown in the inset.

Figure 2 presents PL spectra of ZnO powders excited by 442 nm laser line in air and vacuum fitted to the sum of 2 Gaussians at about 540 and 640 nm. With irradiation in vacuum PL intensity rapidly increases in nonactivated ZnO powder, due to the increase in the broad green luminescence band at  $\approx 540$  nm, Fig. 2a. This emission attributed to electron transition, mediated by defect levels in the band gap [5], is strongly correlated to the density of singly ionized oxygen vacancies [6] located at the surface [7]. The PL spectra intensity in as-prepared activated ZnO powder, excited by the same energy, increase with activation time [2], with additional increase due to irradiation in vacuum, Fig. 2b. This was expected because the nonstoichiometry of activated ZnO powder is a consequence of both activation and irradiation in the vacuum.

Figure 3 presents PL spectra of the ZnO powders excited by the UV line of a He–Cd laser with a wavelength of 325 nm (3.81 eV) in air and vacuum. The spectra of nonactivated ZnO powder show strong emission peak at about 410 nm, with increasing intensity due to irradiation in vacuum. This violet luminescence probably originates from radiative defects related to oxygen vacancies. However, activated samples exhibit weak luminescence, both in UV and violet spectral ranges. As ZnO powders have luminescence in green and yellow/orange spectral region, PL spectra in visible range are fitted to the sum of 2 corresponding Gaussians. The intensity in this PL decreases with activation time [2], while there is no significant change in these spectra due to irradiation in vacuum. This indicates that oxygen vacancy complexes, as specific defects, are not a green luminescence center in ZnO excited by UV light; they may in fact act as the quenching centers [8].

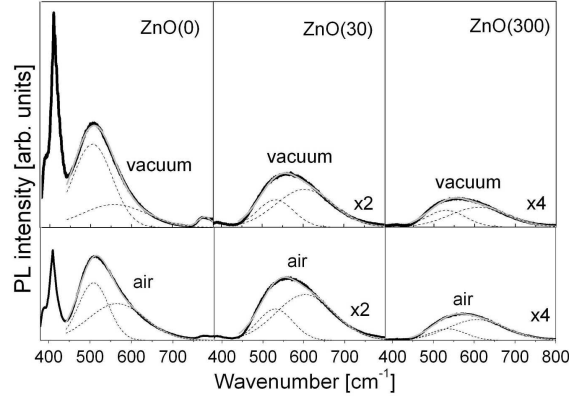


Fig. 3. PL spectra of nonactivated ZnO powder (ZnO(0)) and ZnO powder activated for 30 (ZnO(30)) and 300 min (ZnO(300)), excited by 325 nm He–Cd laser line, in air and vacuum, fitted to the sum of 2 Gaussians.

### 3.2. $TiO_2$

Raman spectra of  $TiO_2$  nanopowder in the air and vacuum, presented in Fig. 4a, confirm its anatase phase in both environments. The observed modes are assigned to the Raman spectrum of anatase single crystal: 145 ( $E_g$ ), 197 ( $E_g$ ), 399 ( $B_{1g}$ ), 513 ( $A_{1g}$ ), 519 ( $B_{1g}$ ), and 639  $cm^{-1}$  ( $E_g$ ) [9]. Laser irradiation in vacuum causes great intensity decrease in the Raman spectrum and small blueshift and broadening of  $E_g$  mode. These changes can be ascribed to nonstoichiometry in anatase  $TiO_2$  [10, 11].

Figures 4b and c show the PL spectra of anatase  $TiO_2$  nanopowder excited by 457.9 nm line of  $Ar^+$  laser with different irradiation times in vacuum and air, respectively. As the visible luminescence of anatase  $TiO_2$  is attributed to 3 different physical origins: oxygen vacancies, surface states and self-trapped excitons [12, 13], the spectra are fitted by a sum of 3 Gaussian modes at about 1.95, 2.20, and 2.40 eV, respectively. Dependence of intensities of these Gaussians on the irradiation time in vacuum and air is presented in Fig. 4d. The intensity of all modes is greater in vacuum than in air, resulting in overall PL intensity increase with irradiation time in vacuum, and subsequent decrease in air. However, the position of PL maximum depends on the relative intensity of those 3 modes. Its redshift in vacuum can be related to the *greatest* increase in PL mode attributed to oxygen vacancies.

## 4. Conclusion

Nonstoichiometry in ZnO powders induced by mechanical activation and laser irradiation in vacuum has a great influence on the PL spectra, depending on activation time and laser excitation energy. It causes the prominent changes both in the PL intensity and position in the spectra excited by visible line of He–Cd

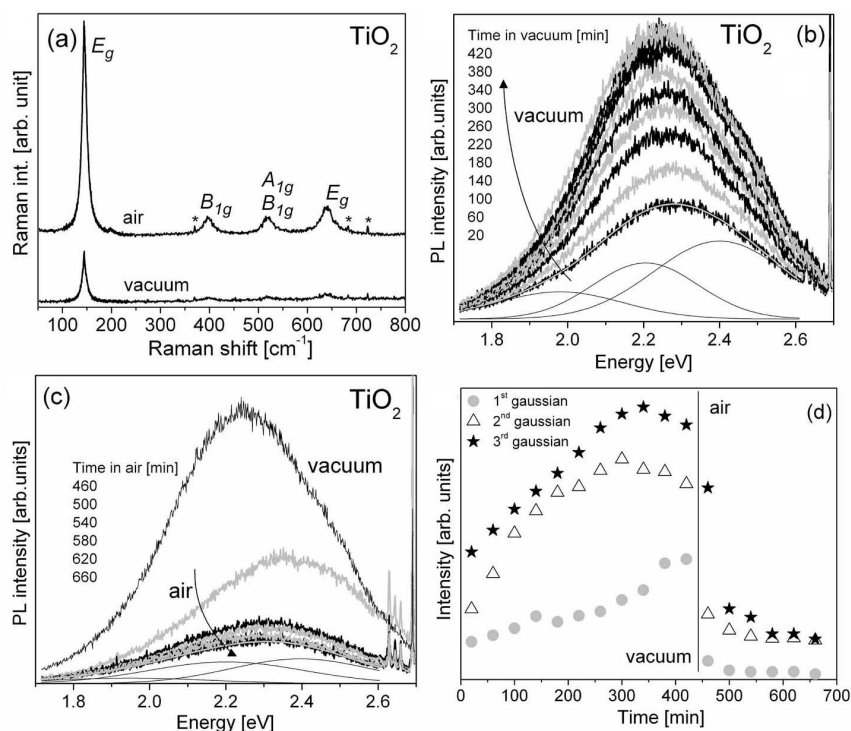


Fig. 4. (a) Raman spectra of anatase TiO<sub>2</sub> nanopowder in air and vacuum (\* — plasma lines). PL spectra of TiO<sub>2</sub> nanopowder in vacuum (b) and air (c), excited by 457.9 nm Ar<sup>+</sup> laser line, with Gaussian intensity of PL bands (d).

laser. These changes are related to the enormous increase in green luminescence excited by visible light, which is strongly correlated to the density of oxygen vacancies located at the surface. Drastic decrease in PL intensity excited by UV line of He–Cd laser in activated ZnO suggests that the surface defects introduced by mechanical activation may act as quenching centers for such luminescence. Different behavior of green luminescence excited by visible and UV light after laser irradiation in vacuum indicates that it can originate from different defect-related transitions depending on the excitation energy.

The observed visible broad-band luminescence in anatase TiO<sub>2</sub> nanopowder is decomposed into 3 PL bands originating from oxygen vacancies, surface states, and self-trapped excitons. These bands are very sensitive to the surface defects introduced by oxygen deficiency. Therefore the intensity and position of the complex PL band are determined by intensities of particular bands and they are strongly dependent on irradiation conditions.

This study confirms crucial role of surface defects, especially oxygen vacancies, in the optical properties of oxide nanopowders and shows how these properties could be changed by preparation and laser irradiation under different conditions.

### Acknowledgments

This work was supported by the MSRS under the projects No. 141047 and 142040 and the OPSA-026283 project within EC FP6 Programme.

### References

- [1] M.A. Hines, P. Guyot-Sionnest, *J. Phys. Chem.* **100**, 468 (1996).
- [2] M. Šćepanović, T. Srećković, K. Vojisavljević, M.M. Ristić, *Sci. Sint.* **38**, 169 (2006).
- [3] C.A. Arguello, D.L. Rousseau, S.P.S. Porto, *Phys. Rev.* **181**, 1351 (1969).
- [4] J.M. Calleja, M. Cardona, *Phys. Rev. B* **16**, 3753 (1977).
- [5] Y. Du, M.-S. Zhang, J. Hong, Y. Shen, Q. Chen, Z. Yin, *Appl. Phys. A* **76**, 171 (2003).
- [6] K. Vanheusden, C.H. Seager, W.L. Warren, D.R. Tallant, J.A. Voigt, *Appl. Phys. Lett.* **68**, 403 (1996).
- [7] D. Li, Y.H. Leung, A.B. Djurišić, Z.T. Liu, M.H. Xie, S.L. Shi, S.J. Xu, W.K. Chan, *Appl. Phys. Lett.* **85**, 1601 (2004).
- [8] T. Ohsaka, F. Izumi, Y. Fujiki, *J. Raman Spectrosc.* **7**, 321 (1978).
- [9] J.C. Parker, R.W. Siegel, *Appl. Phys. Lett.* **57**, 943 (1990).
- [10] M.J. Šćepanović, M.U. Grujić-Brojčin, Z.D. Dohčević-Mitrović, Z.V. Popović, *Mater. Sci. Forum* **518**, 101 (2006).
- [11] T. Sekiya, S. Kamei, S. Kurita, *J. Lumin.* **87-89**, 1140 (2000).
- [12] Y. Lei, L.D. Zhang, G.W. Meng, G.H. Li, X.Y. Zhang, C.H. Liang, W. Chen, S.X. Wang, *Appl. Phys. Lett.* **78**, 1125 (2001).
- [13] K. Vanheusden, C.H. Seager, W.L. Warren, D.R. Tallant, J. Caruso, M.J. Hampden-Smith, T.T. Kodas., *J. Lumin.* **75**, 11 (1997).